

Targeted Genome Modification in Mice Using Zinc-Finger Nucleases

Iara D. Carbery,* Diana Ji,* Anne Harrington,[†] Victoria Brown,*
Edward J. Weinstein,* Lucy Liaw[†] and Xiaoxia Cui*¹

*Sigma Advanced Genetic Engineering Labs, Sigma-Aldrich Biotechnology, St. Louis, Missouri 63146
and [†]Maine Medical Center Research Institute, Scarborough, Maine 04074

Manuscript received March 26, 2010
Accepted for publication June 24, 2010

ABSTRACT

Homologous recombination-based gene targeting using *Mus musculus* embryonic stem cells has greatly impacted biomedical research. This study presents a powerful new technology for more efficient and less time-consuming gene targeting in mice using embryonic injection of zinc-finger nucleases (ZFNs), which generate site-specific double strand breaks, leading to insertions or deletions via DNA repair by the nonhomologous end joining pathway. Three individual genes, multidrug resistant 1a (*Mdr1a*), jagged 1 (*Jag1*), and notch homolog 3 (*Notch3*), were targeted in FVB/N and C57BL/6 mice. Injection of ZFNs resulted in a range of specific gene deletions, from several nucleotides to >1000 bp in length, among 20–75% of live births. Modified alleles were efficiently transmitted through the germline, and animals homozygous for targeted modifications were obtained in as little as 4 months. In addition, the technology can be adapted to any genetic background, eliminating the need for generations of backcrossing to achieve congenic animals. We also validated the functional disruption of *Mdr1a* and demonstrated that the ZFN-mediated modifications lead to true knockouts. We conclude that ZFN technology is an efficient and convenient alternative to conventional gene targeting and will greatly facilitate the rapid creation of mouse models and functional genomics research.

CONVENTIONAL gene targeting technology in mice relies on homologous recombination in embryonic stem (ES) cells to target specific gene sequences, most commonly to disrupt gene function (DOETSCHMAN *et al.* 1987; KUEHN *et al.* 1987; THOMAS and CAPECCHI 1987). Advantages of gene targeting in ES cells are selective target sequence modification, the ability to insert or delete genetic information, and the stability of the targeted mutations through subsequent generations. There are also potential limitations, including limited rates of germline transmission and strain limitations due to lack of conventional ES cell lines (LEDERMANN 2000; MISHINA and SAKIMURA 2007). Moving the targeted allele from one strain to another requires 10 generations of backcrosses that take 2–3 years. A minimum of 1 year is necessary for backcrossing if speed congenics is applied (MARKEL *et al.* 1997).

Zinc-finger nucleases (ZFNs) are fusions of specific DNA-binding zinc finger proteins (ZFPs) and a nuclease domain, such as the DNA cleavage domain of a type II endonuclease, *FokI* (KIM *et al.* 1996; SMITH *et al.* 1999; BIBIKOVA *et al.* 2001). A pair of ZFPs provide target specificity, and their nuclease domains dimerize to

cleave the DNA, generating double strand breaks (DSBs) (MANI *et al.* 2005), which are detrimental to the cell if left unrepaired (RICH *et al.* 2000). The cell uses two main pathways to repair DSBs: high-fidelity homologous recombination and error-prone nonhomologous end joining (NHEJ) (LIEBER 1999; PARDO *et al.* 2009; HUERTAS 2010). ZFN-mediated gene disruption results from deletions or insertions frequently introduced by NHEJ. Figure 1 illustrates the cellular events following the injection of a pair of ZFNs targeting the mouse *Mdr1a* (also known as *Abcb1a*) gene.

ZFNs have been successfully applied to generate genome modifications in plants (SHUKLA *et al.* 2009; TOWNSEND *et al.* 2009), fruit flies (BIBIKOVA *et al.* 2002), *Caenorhabditis elegans* (MORTON *et al.* 2006), cultured mammalian cells (PORTEUS and BALTIMORE 2003; SANTIAGO *et al.* 2008), zebrafish (DOYON *et al.* 2008; MENG *et al.* 2008), and most recently in rats (GEURTS *et al.* 2009; MASHIMO *et al.* 2010). The technology is especially valuable for rats because rat ES cell lines have only become available recently (BUEHR *et al.* 2008; LI *et al.* 2008), and successful homologous recombination-mediated genome modification has not been reported. Previously, ENU mutagenesis (ZAN *et al.* 2003) or transposons (KITADA *et al.* 2007) were the two main methods for generating gene knockout rats, both of which are random approaches and require labor-intensive and time-consuming screens to obtain the desired gene disruptions.

Supporting information is available online at <http://www.genetics.org/cgi/content/full/genetics.110.117002/DC1>.

¹Corresponding author: 2033 Westport Center Dr., St. Louis, MO 63146.
E-mail: xiaoxia.cui@sial.com

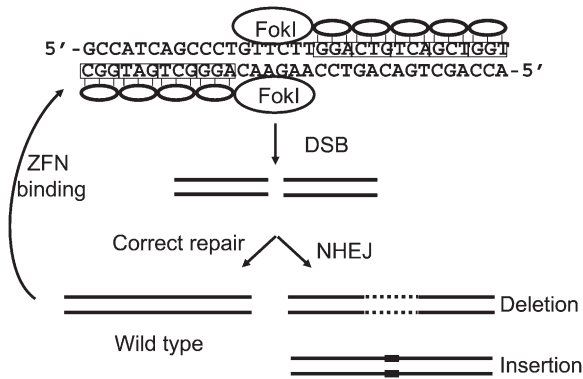


FIGURE 1.—The ZFN targeting mechanism. ZFN pairs bind to the target site, and *FokI* endonuclease domain dimerizes and makes a double strand break between the binding sites. If a DSB is repaired so that the wild-type sequence is restored, ZFNs can bind and cleave again. Otherwise, nonhomologous end joining (NHEJ) introduces deletions or insertions, which change the spacing between the binding sites so that ZFNs might still bind but dimerization or cleavage cannot occur. Insertions or deletions potentially disrupt the gene function.

Although ES cell-based knockout technology is widely used in mice, ZFN technology offers three advantages: (i) high efficiency; (ii) drastically reduced timeline, similar to that of creating a transgene (GORDON *et al.* 1980); and (iii) the freedom to apply the technology in various genetic backgrounds. In addition, no exogenous sequences need to be introduced because selection is not necessary.

Here, we created the first genome-engineered mice using ZFN technology. Three genes were disrupted in two different backgrounds: *Mdr1a*, *Jag1*, and *Notch3* in the FVB/N strain and *Jag1* also in the C57BL/6 strain. All founders tested transmitted the genetic modifications through the germline.

MATERIALS AND METHODS

In vitro preparation of ZFN mRNAs: The ZFN expression plasmids were obtained from Sigma's CompoZr product line. Each plasmid was linearized at the *XbaI* site, which is located at the 3' end of the *FokI* ORF. 5' capped and 3' poly(A)-tailed message RNA was prepared using either MessageMax T7 capped transcription kit and poly(A) polymerase tailing kit (Epicentre Biotechnology, Madison, WI) or mMessage (mMachine) T7 kit and poly(A) tailing kit (Ambion, Austin, TX). The poly(A) tailing reaction was precipitated with an equal volume of 5 M NH_4OAc and then dissolved in injection buffer (1 mM Tris-HCl, pH 7.4, 0.25 mM EDTA). mRNA concentration was estimated using a NanoDrop 2000 Spectrometer (Thermo Scientific, Wilmington, DE).

ZFN validation in cultured cells: National Institutes of Health (NIH) 3T3 cells were grown in DMEM with 10% FBS and antibiotics at 37° with 5% CO_2 . ZFN mRNAs were paired at 1:1 ratio and transfected into the NIH 3T3 cells to confirm ZFN activity using a Nucleofector (Lonza, Basel, Switzerland), following the manufacturer's 96-well shuttle protocol for 3T3 cells. Twenty-four hours after transfection, culturing medium was removed, and cells were incubated with 15 μl of trypsin per well for 5 min at 37°. The cell suspension was then transferred

to 100 μl of QuickExtract (Epicentre) and incubated at 68° for 10 min and 98° for 3 min. The extracted DNA was then used as template in a PCR reaction to amplify 350- to 650-bp amplicons around the target site with the following primer pairs: *Mdr1a* Cel-I F, ctgtttcttgacaaaacaacactaggctc; *Mdr1a* Cel-I R, gggctcagggaagagttttaaatac; *Jag1* Cel-I F, ctctggggcactgtcttag; *Jag1* Cel-I R, gcgggactgatactccttga; *Notch3* Cel-I F, tttaagtgggcgcttctgg; and *Notch3* Cel-I R, ggcagaggtactgttcacc.

Each 50- μl PCR reaction contained 1 μl of template, 5 μl of buffer II, 5 μl of 10 μM each primer, 0.5 μl of AccuPrime Taq polymerase high fidelity (Invitrogen, Carlsbad, CA), and 38.5 μl of water. The following PCR program was used: 95°, 5 min, 35 cycles of 95°, 30 sec, 60°, 30 sec, and 68°, 45 sec, and then 68°, 5 min. Three microliter of the above PCR reaction was mixed with 7 μl of 1 \times buffer II and incubated under the following program: 95°, 10 min, 95° to 85° at $-2^\circ/\text{s}$, 85° to 25° at $-0.1^\circ/\text{s}$.

One microliter each of nuclease S (Cel-I) and enhancer (Transgenomic, Omaha, NE) were added to digest the above reaction at 42° for 20 min. The mixture is resolved on a 10% polyacrylamide TBE gel (Bio-Rad, Hercules, CA).

Microinjection and mouse husbandry: FVB/NTac and C57BL/6NTac mice were housed in static cages and maintained on a 14 hr/10 hr light/dark cycle with *ad libitum* access to food and water. Three- to 4-week-old females were injected with PMS (5 IU/mouse) 48 hr before hCG (5 IU/mouse) injection. One-cell fertilized eggs were harvested 10–12 hr after hCG injection for microinjection. ZFN mRNA was injected at 2 ng/ μl . Injected eggs were transferred to pseudopregnant females [Swiss Webster (SW) females from Taconic Labs mated with vasectomized SW males] at 0.5 days post coitum (dpc).

Founder identification using mutation detection assay: Toe clips were incubated in 100–200 μl of QuickExtract (Epicentre Biotechnology) at 50° for 30 min, 65° for 10 min, and 98° for 3 min. PCR and mutation detection assay were done under the same conditions as in ZFN validation in cultured cells using the same sets of primers.

TA cloning and sequencing: To identify the modifications in founders, the extracted DNA was amplified with Sigma's JumpStart Taq ReadyMix PCR kit. Each PCR reaction contained 25 μl of 2 \times ReadyMix, 5 μl of primers, 1 μl of template, and 19 μl of water. The same PCR program was used as in ZFN validation in cultured cells. Each PCR reaction was cloned using TOPO TA cloning kit (Invitrogen) following the manufacturer's instructions.

At least eight colonies were picked from each transformation, PCR amplified with T3 and T7 primers, and sequenced with either T3 or T7 primer. Sequencing was done at Elim Biopharmaceuticals (Hayward, CA).

PCR for detecting large deletions: To detect larger deletions, which removed the original Cel-I priming sites, another set of distal primers were used for each of the targets: *Mdr1a* 800F, catgctgtgaagcagatacc; *Mdr1a* 800R, ctgaaactgaatgagacatttc; *Jag1* 600F, ggtgggaactggaagtagca; *Jag1* 600R, ggagtctctctccgctctt; *Notch3* 800F, tctcaacaaccacaacca; and *Notch3* 800R, gtcgtctgcaagagcaagtgc.

Each 50- μl PCR contained: 1 μl of template, 5 μl of 10 \times buffer II, 5 μl of 10 μM of each 800F/R primer, 0.5 μl of AccuPrime Taq polymerase high fidelity (Invitrogen), and 38.5 μl of water. The following program was used: 95°, 5 min, 35 cycles of 95°, 30 sec, 60°, 30 sec, and 68°, 3 min, and then 68°, 5 min. The samples were resolved on a 1% agarose gel. Distinct bands with lower molecular weight than the wild type (WT) were sequenced.

RNA preparation from tissues and RT-PCR: *Mdr1a*^{-/-} or *Mdr1a*^{+/+} littermates were sacrificed for tissue harvest at 5–9 weeks of age. Large intestine, kidney, and liver tissues were dissected and immediately used or stored in RNAlater solution

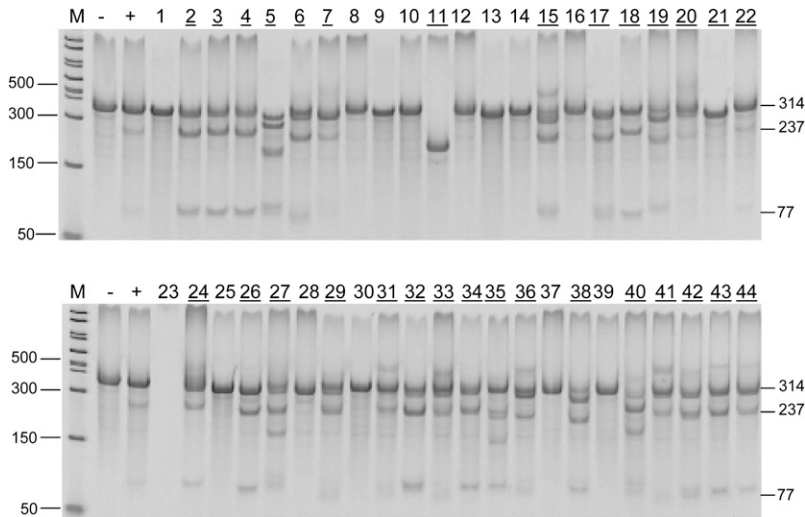


FIGURE 2.—Identification of genetically engineered *Mdr1a* founders using the *Cel-I* mutation detection assay. Cleaved bands indicate a mutation is present at the target site (see MATERIALS AND METHODS). Bands are marked with respective sizes in base pairs. M, PCR marker. One to 44 pups born from injected eggs. The numbers representing the mutant founder animals are underlined.

(Ambion) at -20° . Total RNA was prepared using GenElute Mammalian Total RNA Miniprep kit (Sigma) following manufacturer's instructions. To eliminate any DNA contamination, the RNA was treated with DNaseI (New England Biolabs, Ipswich, MA) before being loaded onto the purification columns.

Mdr1a RT-PCR analysis was carried out with 1 μ l of total RNA, primers RT-F (5'-GCCGATAAAAGAGCCATGTTTG) and RT-R (5'-GATAAGGAGAAAAGCTGCACC), using SuperScript III one-step RT-PCR system with platinum Taq high fidelity kit (Invitrogen). Reverse transcription and subsequent PCR were carried out with 1 cycle of 55° for 30 min and 94° for 2 min for cDNA synthesis and 40 cycles of 94° for 15 sec, 56° for 30 sec, and 68° for 1 min for amplification. The PCR product was loaded in a 1.2% agarose gel and visualized with ethidium bromide. Nested PCR used primers RT-F2 (5'-CTGGAGGAA GAAATGACCACG) and RT-R2 (5'-GATAGCTTTCTTTATCC CCAGCC).

Western blot analysis: Mice were killed and the large intestine was immediately harvested and flushed with ice-cold PBS buffer, snap frozen on dry ice, and stored at -80° . For protein preparation, tissue pieces equivalent to ~ 200 μ l were shaved off the frozen samples and placed into an ice-cold microcentrifuge tube. Four hundred microliters of ice-cold PBS with $4\times$ protease inhibitors was added, and the sample was dounce homogenized. The homogenate was pelleted at $20,000 \times g$ for 5 min at 4° , and the supernatant (S1) was removed. The pellet, after being resuspended in 400 μ l of ice-cold PBS with $4\times$ protease inhibitors, was centrifuged at $4000 \times g$ for 5 min at 4° . The supernatant (S2) was removed, and the pellet was resuspended in 500 μ l lysis buffer (composition) (GERLACH *et al.* 1987), dounce homogenized, incubated on ice for 40 min with intermittent vortexing for 15 sec per interval, and finally pelleted at $20,000 \times g$ for 20 min at 4° . The supernatant (S3) was collected, and the pellet was resuspended again in 250 μ l of lysis buffer, dounce homogenized, spun at $4000 \times g$ for 5 min at 4° , and the supernatant (S4) was kept. The S3 and S4 fractions were diluted 1:1 with $2\times$ Laemmli buffer (Sigma) and incubated at 37° for 5–10 min. Lysates (15 μ l, 10 μ l, or 5 μ l) were separated on a 4–20% Mini-PROTEAN TGX precast gel (BioRad) and transferred to nitrocellulose membrane using a semi-dry transblot (BioRad) at 25 V for 1 hr. The transfer buffer contained standard tris-glycine salts, 18% MeOH, and 0.25% SDS. Mouse anti-*Mdr1a* antibody C219 (Covance, Princeton, NJ) at 1:100 and mouse anti-actin antibody at 1:1000 (Sigma) were incubated together with the blot overnight in 5% milk/TBST, rocking at 4° , rinsed

briefly in TBST, and the HRP-conjugated goat anti mouse secondary antibody (Jackson ImmunoResearch Labs, West Grove, PA) was incubated for 1 hr in 1% milk/TBST following a quick rinse with TBST, followed by 2×50 ml washes of 1% milk/TBST for 10 min. HRP was detected using the SuperSignal West Pico substrate (Thermo) and a ChemiDocXRS+ imaging system (Bio-Rad).

RESULTS

ZFN injection resulted in high-efficiency knockout at the *Mdr1a* locus: Validated *Mdr1a* ZFN mRNA (supporting information, Figure S1, File S1, and MATERIALS AND METHODS) was microinjected into fertilized FVB/N eggs, which were transferred into pseudopregnant females. Pups born from the injected embryos were tested using a DNA mismatch endonuclease (*Cel-I*) assay (see MATERIALS AND METHODS) for modifications at the target site. Thirty of the 44 live births contained deletions or insertions. Figure 2 shows the founders among wild-type littermates.

Larger deletions generated by ZFN activity: Some of the samples yielded no amplification product with the *Cel-I* primers. To detect potentially larger deletions that would have destroyed the priming sites used in Figure 2, a larger region spanning 800 bp on both sides of the cleavage site was PCR amplified. Figure 3 shows that 15 of the 44 pups indeed contain larger deletions, including 4 animals that were not identified as founders by the previous PCR assay. The PCR products for all founders were TA cloned and sequenced to reveal the exact sequences of modifications, and the deletions ranged between 3 and 731 bp in length as well as some small insertions (Table S1). Interestingly, three small deletions were each found in two or more founders: a 19-bp deletion in founders 7, 17, and 36, a 21-bp deletion in founders 17 and 20, and a 6-bp deletion in founders 34 and 44 (Figure S2). All three deletions are flanked by a 2-bp microhomology, which is predicted to create a common NHEJ junction (LIEBER 1999).

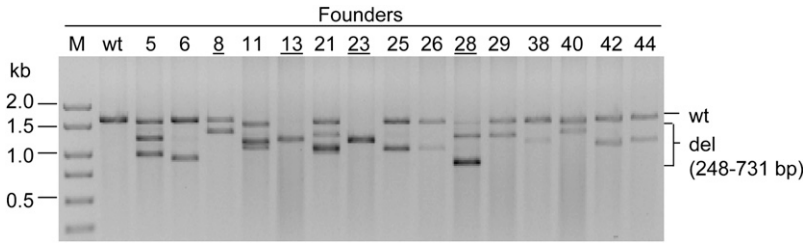


FIGURE 3.—Large deletions in *Mdr1a* founders. PCR products were amplified using primers located 800 bp upstream and downstream of the ZFN target site. Bands significantly smaller than the 1.6-kb wild-type band indicate large deletions in the target locus. Four founders that were not identified in Figure 2 are underlined.

High rate of germline transmission by *Mdr1a* founders: Nine of the founders were chosen to back-cross to the wild-type FVB/N mice to the F₁ generation, all of which transmitted at least one mutant allele to their offspring. Seven founders transmitted more than two mutated alleles. Interestingly, in some cases, alleles that were not initially identified in the founders were also transmitted through the germline and discovered in the next generation, such as in founders 6, 8, 13, 21, and 44 (Table S2), most likely due to incomplete sequencing of the TA clones (see DISCUSSION).

***Mdr1a* expression by RT-PCR and Western:** The *Mdr1a* protein is differentially expressed in tissues. Liver

and large intestine predominantly express *Mdr1a*, and kidney expresses both *Mdr1a* and *Mdr1b* (SCHINKEL *et al.* 1994). To verify that a deletion in the *Mdr1a* gene abolishes its expression, we performed RT-PCR on total RNA from liver, kidney, and intestine of *Mdr1a*^{-/-} mice established from founder 23, with a 396-bp deletion (Figure 4A), using a forward and a reverse primer located in exons 5 and 9, respectively. Samples from all the *Mdr1a*^{-/-} tissues produced a smaller product with lower yield than those of corresponding wild-type samples, with a sequence correlating to exon 7 skipping and subsequent multiple premature stop codons in exon 8 in the mutant animals (Figure 4B). Furthermore,

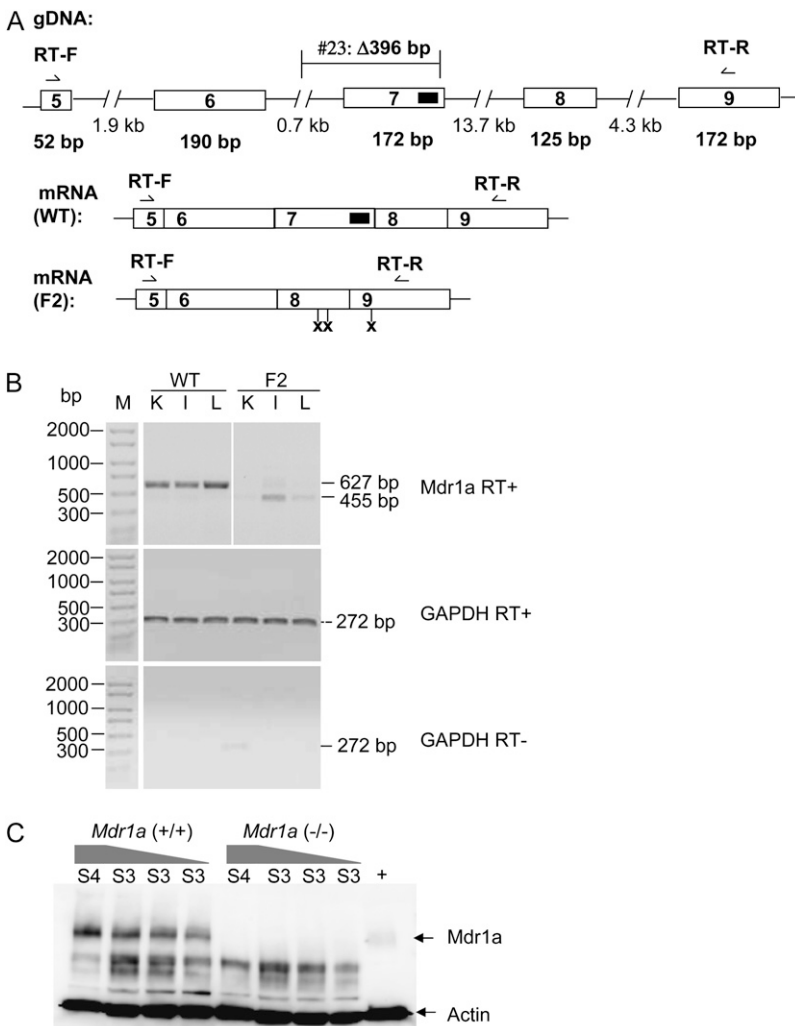


FIGURE 4.—*Mdr1a* expression in homozygous knockout animals. (A) A schematic of *Mdr1a* genomic and mRNA structures around the ZFN target site in exon 7, marked with a solid black rectangle. Exons are represented by open rectangles with respective numbers. The size of each exon in base pairs is labeled directly underneath it. Intron sequences are represented by broken bars with size in base pairs underneath. The position of the 396-bp deletion in founder 23 is labeled above intron 6 and exon 7. RT-F and RT-R are the primers used in RT-PCR, located in exons 5 and 9, respectively. (B) *Mdr1a* expression in tissues. For RT reactions, 40 ng of total RNA was used as template. Normalization of the input RNA was confirmed by *GAPDH* amplification with or without reverse transcriptase. M, PCR marker; WT, wild-type mouse; F2, *Mdr1a*^{-/-} mouse; K, kidney; I, large intestine; L, liver. Amplicon sizes are marked on the right. (C) Western blot analysis with large intestine. +, positive control, lysate from the human *Mdr1*-overexpressing SK-N-FI cells (ATCC, Manassas, VA). S3 (15 μ l, 10 μ l, and 5 μ l loaded in each of the three lanes) and S4 (15 μ l loaded), the third and fourth supernatant fractions of large intestine membrane preparations (see MATERIALS AND METHODS). Actin was used as a loading control. *Mdr1a*^{+/+}, wild-type intestine; *Mdr1a*^{-/-}, intestine from a homozygous knockout mouse derived from founder 23.

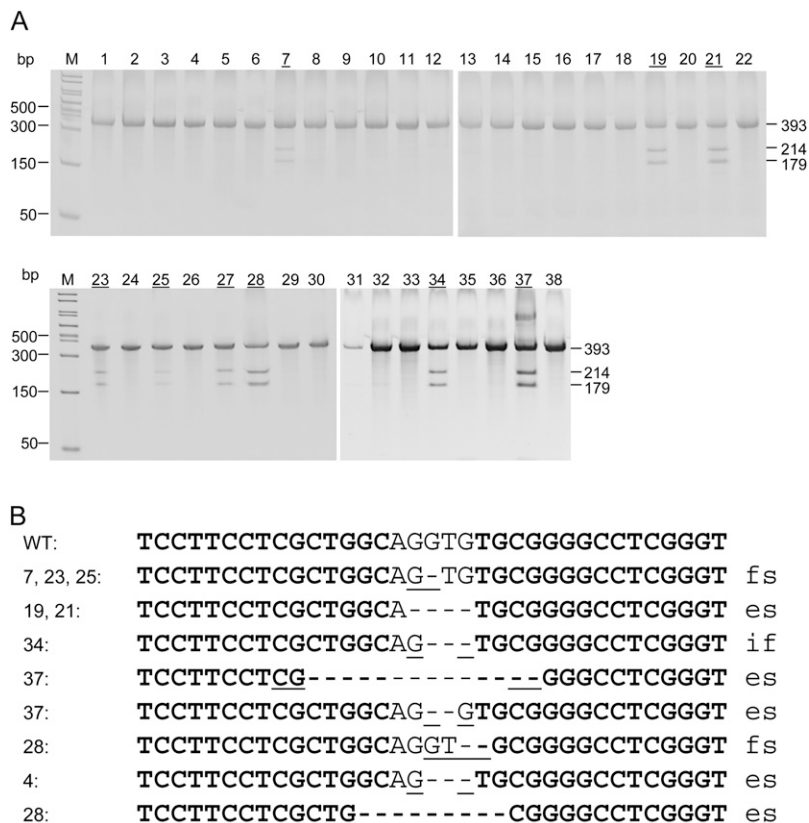


FIGURE 5.—Identification and genotype of *Jag1* founders. (A) *Jag1* founders identified using the *Cel-I* mutation detection assay. M, PCR marker; 1–38, pups born from two injection sessions. The numbers of founders are underlined. The sizes in base pairs of uncut and cut bands are labeled on the right. (B) Genotype of the *Jag1* founders. Target site sequences of wild type and founders are aligned. ZFN binding sites are in boldface type. A dash represents a deleted nucleotide. One to 4 bp of microhomology that was likely used by NHEJ is underlined. The frameshift (fs), exon skipping (es), or in-frame amino acid loss (if) resulting from each deletion is indicated to the right of each sequence.

Western blotting with an anti-Mdr1a antibody showed absence of Mdr1a protein in the large intestine of *Mdr1a*^{-/-} animals (Figure 4C), demonstrating that the 396-bp deletion leads to a true knockout.

High-efficiency targeting and germline transmission in C57BL/6 strain: Next, we microinjected *Jag1* ZFN mRNA into fertilized eggs from C57BL/6 strain and identified 24% founders among live births (Figure 5A). The *Jag1* ZFNs precisely target the junction of intron 1 and exon 2; therefore, even small deletions can destroy the recognition site for splicing. Deletions among *Jag1* founders range from 1 to 14 bp (Figure 5B). Five founders, 4, 19, 21, 28, and 37, carry deletions that mutated the conserved G residue at the end of the intron and will likely lead to exon 2 skipping and deletion of 102 amino acids from the protein. Except for founders 28 and 37, both with two mutant alleles, the rest of the founders only bear one mutated allele. Similar to some *Mdr1a* founders, some *Jag1* founders carry the same deletions. Founders 7, 23, and 25 share the same 1-bp deletion. Founders 19 and 21 bear the same 4-bp deletion. Except for the mutant allele in founders 19 and 21, the rest of the deletions are flanked by 1- to 2-bp microhomology (Figure 5B, also see DISCUSSION). Founder 28 has a 2-bp deletion, both resulting in frameshift and premature stop codons shortly downstream. Founder 19 was backcrossed to wild-type C57BL/6 and achieved germline transmission in the first mating (three heterozygotes among eight F₁ pups).

Notch3 targeting in FVB/N mice: We targeted a third gene, *Notch3*, again in FVB/N and obtained 20% founder rate (Figure 6A). Founders 1 and 2 have large deletions, 367 bp and 1121 bp, respectively (Figure 6B). Number 9 is the only founder carrying two different mutated alleles, a 1-bp deletion, and an 8-bp deletion. Again, the same 8-bp deletion in founder 9 was also identified in founders 13 and 23, and founders 8 and 26 both carry an identical 16-bp deletion. All three deletions are flanked by a 2-bp microhomology (Figure 6C, also see DISCUSSION). All deletions are completely within exon 11, resulting in a frameshift that introduces premature translational stop codons within the exon.

Potential off-target sites validation: We identified 20 sites in the mouse genome that are most similar to the *Mdr1a* target site, all with 5-bp mismatches from the ZFN binding sequence, and top potential off-target sites for *Jag1* and *Notch3*, all with at least 6-bp mismatches from their respective target sites (Table S3, Table S4, and Table S5). To validate specificity of the *Mdr1a* ZFNs, we tested the site in the *Mdr1b* gene, which is 88% identical to *Mdr1a*, in all 44 *Mdr1a* F₀ pups using mutation detection assay. None of the 44 pups had an NHEJ event at the *Mdr1b* site (Figure S3). To further and more fully characterize the *Mdr1a* mutant animals, we tested all the predicted potential off-target sites in four founder animals and found no spurious mutations (Figure S4).

DISCUSSION

We generated mice with modifications at three loci by direct injection of ZFN mRNA into the pronucleus of one-cell mouse embryos. ZFN technology offers a few obvious advantages when compared to conventional methods in producing knockout mice. By bypassing ES cells, ZFN technology enables the generation of homozygous mice with targeted modifications in a matter of months, with no need for selection. Highly efficient targeting (20–75%) allows one to identify founders by screening relatively small number of pups. Many founders carry more than one mutant allele in addition to the wild-type allele, implying that ZFNs remain active beyond one-cell stage. Every cell division doubles the number of the wild-type allele, which is the only allele cleavable by ZFNs. Deletions or insertions change the space between ZFN binding sites, preventing *FokI* domains from dimerization. For those founders harboring up to five different alleles, ZFN-mediated cleavage likely did not happen before the first embryonic cell division. Thus, most founders are mosaics. All tested founders transmitted at least one mutant allele through the germline (Table S1).

Most *Mdr1a* founders transmitted more than one allele, as observed in rats as well (GEURTS *et al.* 2009). Some alleles that were not identified in the founders were inherited in F₁ generation (Table S2), which was likely caused by PCR bias and incomplete sampling of the TA clones. PCR reactions for detecting large deletions, which favor amplification of smaller products resulting from larger deletions, were used to TA clone, followed by sequencing to identify mutant alleles. We only sequenced 8–16 clones from each founder. Some of the small deletions, especially if they were also low representing, could be missed. Although all live births were tested with Cel-I assay (with a detection limit ~1%), some of the negative pups may carry low-representing alleles that are still germline competent. It is also possible that toe or tail clips do not necessarily have the same genotype as germ cells, of which we observed only one confirmed example. Founder 23 did not have wild-type allele amplification in either toe or tail DNA. Yet when mated to wild-types, only 50% of its F₁'s were heterozygous. The other half was wild type. Thus wild-type allele was present in the germline but was not represented in the toe or tail samples we analyzed.

We examined the effect of modifications on gene expression in one of the *Mdr1a*^{-/-} strains in further detail. The RT-PCR results demonstrate that the samples from the *Mdr1a*^{-/-} founder 23 produce a transcript missing the 172-bp exon 7 that causes exon skipping during mRNA splicing and immediately creates multiple premature translational stop codons in the message (Figure 4B). Such mutations often lead to nonsense-mediated decay (NMD) of the mutant mRNA (CHANG *et al.* 2007), and this is supported by an apparently

reduced level of exon-skipping transcript, compared to that of the wild type, detected in RT-PCR analyses (Figure 4B), implying likely mRNA degradation provoked by NMD. In the *Mdr1a*^{-/-} samples, there were faint bands at and above the size of the wild-type transcript, which are most likely PCR artifacts because amplification of those bands excised from the gel yielded mostly the exon-skipped product. The bands at the wild-type size in secondary rounds of PCR were mixtures that did not yield readable sequences (not shown). This conclusion is supported by Western blot analysis using an anti-Mdr1a antibody that detected abundant protein expression in the large intestine (which highly expresses Mdr1a but not Mdr1b) of wild-type littermates but no detectable Mdr1a protein in the same tissue of homozygous animals derived from founder 23. Thus, the *Mdr1a*^{-/-} mice derived from founder 23 represent a functional knockout. Consistent with the theory of possible NMD, we obtained similar RT-PCR results on another animal, a compound homozygote from founder 11, harboring 417- and 533-bp deletions in respective alleles. A smaller amplicon corresponding to exon skipping was detected at a lower level than that of wild-type PCR product (not shown), as in the case of *Mdr1a*^{-/-} from founder 23. This observation extends to the rat as well. A 19-bp deletion in the rat *Mdr1a* locus, greatly reduced the mRNA level, though sizewise it was similar to the wild-type and again, Western blots showed complete lack of Mdr1a expression in *Mdr1*^{-/-} large intestine (I. D. CARBERY and X. CUI, unpublished data).

The mouse *Mdr1a* gene has 28 exons, and the encoded protein is composed of two units of six transmembrane domains (TMs 1–6 and TMs 7–12), each unit with an ATP binding site and with a linker region in between the units (MITZUTANI and HATTORI 2005). All 12 TM domains as well as the two ATP-binding motifs are essential for Mdr1a function (PIPPERT and UMBENHAUER 2001). The *Mdr1a* ZFNs target exon 7, which encodes TMs 3 and 4. On the basis of previous work in this field, any partial protein that might result from the described frameshift and nonsense mutations we observed (assuming such protein fragments could be stable) should not be functional (PIPPERT and UMBENHAUER 2001). Among the mutant alleles, 41% cause exon skipping, 37% result in frameshift, and the rest carry in-frame deletions (Table S1). It is safe to conclude that the majority of the mutants obtained will be true knockouts.

Interestingly, large deletions were introduced in both targets, *Mdr1a* and *Notch3* in the FVB/N strain but not in *Jag1* in C57BL/6, suggesting a possible difference in DNA repair that may be related to the host genetic background. However, injection of *Jag1* ZFNs into FVB/N embryos resulted in similar founder rate and deletion sizes (not shown) as in C57BL/6, indicating the difference in deletion size might not have resulted from variation in genetic background. The *Mdr1a* locus also has a higher percentage of large deletions than

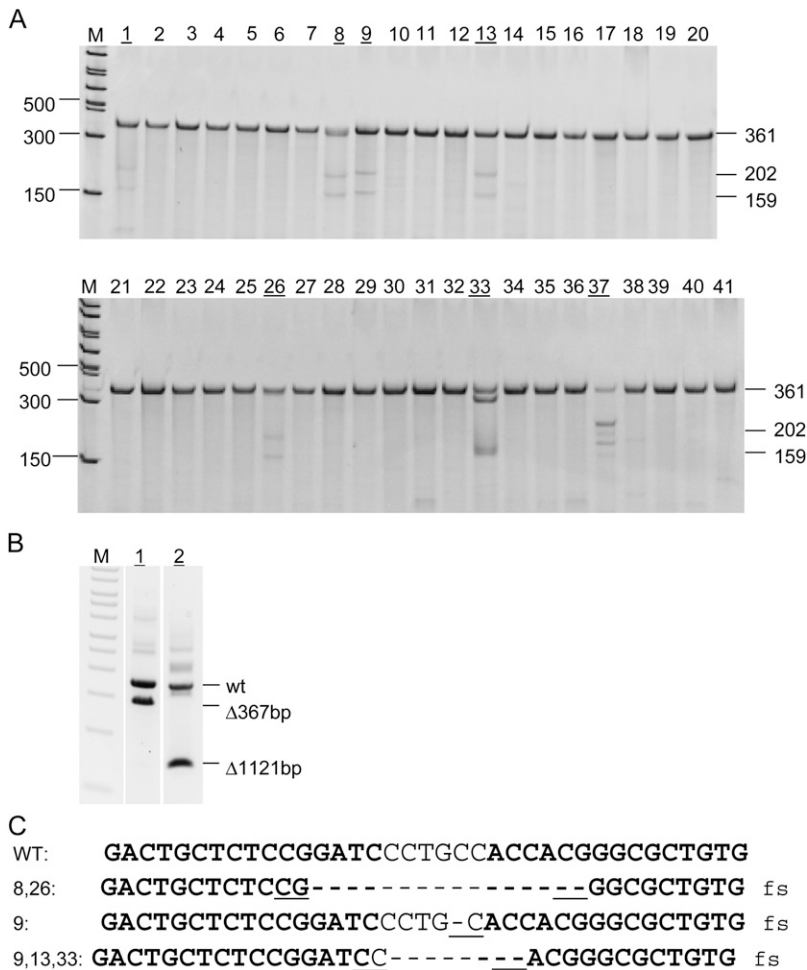


FIGURE 6.—Identification and genotype of *Notch3* founders. M, PCR marker. (A) The *Cel-I* mutation detection assay was used to identify founders, whose numbers are underlined. (B) Large deletions were detected in founders 1 and 2. (C) Genotype of the *Notch3* founders. ZFN binding sites are in boldface type. A dash represents a deleted nucleotide. One to 4 bp of microhomology that was likely used by NHEJ is underlined. All deletions result in frameshift (fs), which is labeled to the right of each sequence.

Notch3, although both were targeted in FVB/N. It is possible that the target site *per se* contributes at least partially to the determination of modifications. Table S6 contains data from all the injections in both FVB/N and C57BL/6, including number of eggs injected, number of pups born from each injection, and number of founders identified among live births. Due to procedural similarity between generation of a transgene and ZFN-mediated genome modifications, any background that is competent for traditional transgenesis should in theory be a good candidate to use for creating a ZFN-mediated knockout. We have not accumulated enough data to analyze differences on targeting efficiency or the types of modifications that can be caused by different mouse backgrounds. However, we and others have observed similar targeting rates in various rat strains, and the size of deletions seems to also be target dependent (SAGE LABS, unpublished data; MASHIMO *et al.* 2010).

Another interesting observation was that for all three targets, some small deletions were identical in multiple founders (Figures 5 and 6 and Figure S2), assuming deletion occurs randomly during NHEJ. We considered the possibility that these deletions were merely PCR artifacts caused by GC-rich microhomology flanking some of the deletions. However, several of the small

deletions transmitted germline (Table S2), proving that these small deletions are true targeting events. Our data support the notion that microhomology of 1–4 bp at the ends of DSBs promotes, but is not necessary for, NHEJ (LIEBER 1999). We noticed that most of the deletions, regardless of whether identified in single or multiple founders, contain 1–4 bp microhomology at the deletion boundary (Figures 5 and 6 and Figure S2). In alleles such as that shared by founders 19 and 21 of *Jag1*, where microhomology is not present, we hypothesize that sequence-dependent DNA secondary structures might form around the target site that pause the resection of the ends by exonucleases before ligation (HUERTAS 2010), so that certain deletions resulted in multiple founders. *Mdr1a*^{-/-} founder 11 contains an unusual allele with discontinuous deletions, a 417-bp deletion from -528 to -112, >100 bp upstream of the cleavage site and flanked by a 5-bp microhomology GACAA, and a 19-bp deletion at the cleavage site, -14 to +5 (Table S1). This complex allele was transmitted through the germline (Table S2). One explanation could be that two sequential ZFN cleavages occurred in the same chromatid. The repair of the first DSB was initiated as homologous recombination using the sister chromatid as template but was completed by NHEJ

using the 5-bp microhomology, as observed previously (RICHARDSON and JASIN 2000), leading to a 417-bp deletion upstream of the target site. The restored target site was cleaved again by ZFNs and repaired by NHEJ, resulting in a 19-bp deletion.

We identified sequences in the mouse genome that are most similar to the *Mdr1a*, *Jag1*, and *Notch3* target sites and tested the potential off-target sites for the *Mdr1a* ZFNs. No modifications were detected at the *Mdr1b* site in any of the 44 live births, and of 80 other off-targets tested (20 sites in four independent founders), none harbored modifications, illustrating the specificity of the *Mdr1a* ZFNs (see Figure S3). Doing the best we could have done without performing costly whole genome sequencing, these data do not exclude that there are off-target sites that do not resemble the target site. Assuming hypothetical, unlinked off-target modifications will be diluted through breeding, an indirect way to detect potential off-target events could be to compare phenotypically early-generation to later-generation homozygotes. The lack of difference in phenotypes implies the absence of off-target events. To include wild-type littermates as controls in phenotyping assays is another way to reduce the possible interference of off-target modifications on phenotype. In the meantime, we do realize that the ultimate proof of absence or presence of off-target events has to come from whole-genome sequencing, which will hopefully be affordable in the near future with the continuous reduction in sequencing cost.

Altogether, we conclude that ZFN technology is a valuable alternative to conventional knockout technology for generating genome modifications in mice.

We thank Fyodor Urnov for helping interpret the puzzling allele in founder 11, Thom Saunders for suggestions on improving mRNA preparation for injection, Dave Briner for ZFN assembly, and Danhui Wang for her assistance in off-target search.

LITERATURE CITED

- BIBIKOVA, M., D. CARROLL, D. J. SEGAL, J. K. TRAUTMAN, J. SMITH *et al.*, 2001 Stimulation of homologous recombination through targeted cleavage by chimeric nucleases. *Mol. Cell Biol.* **21**: 289–297.
- BIBIKOVA, M., M. GOLIC, K. G. GOLIC and D. CARROLL, 2002 Targeted chromosomal cleavage and mutagenesis in *Drosophila* using zinc-finger nucleases. *Genetics* **161**: 1169–1175.
- BUEHR, M., S. MEEK, K. BLAIR, J. YANG, J. URE *et al.*, 2008 Capture of authentic embryonic stem cells from rat blastocysts. *Cell* **135**: 1287–1298.
- CHANG, Y.-F., J. S. IMAM and M. F. WILKINSON, 2007 The nonsense-mediated decay RNA surveillance pathway. *Annu. Rev. Biochem.* **76**: 51–74.
- DOETSCHMAN, T., R. G. GREGG, N. MAEDA, M. L. HOOPER, D. W. MELTON *et al.*, 1987 Targeted correction of a mutant HPRT gene in mouse embryonic stem cells. *Nature* **330**: 576–578.
- DOYON, Y., J. M. MCCAMMON, J. C. MILLER, F. FARAJI, C. NGO *et al.*, 2008 Heritable targeted gene disruption in zebrafish using designed zinc-finger nucleases. *Nat. Biotechnol.* **26**: 702–708.
- GERLACH, J. H., D. R. BELL, C. KARAKOUSIS, H. K. SLOCUM, N. KARTNER, *et al.*, 1987 P-glycoprotein in human sarcoma: evidence for multidrug resistance. *J. Clin. Oncol.* **5**: 1452–1460.
- GEURTS, A. M., G. J. COST, Y. FREYVERT, B. ZEITLER, J. C. MILLER *et al.*, 2009 Knockout rats via embryo microinjection of zinc-finger nucleases. *Science* **325**: 433.
- GORDON, J. W., G. A. SCANGOS, D. J. PLOTKIN, J. A. BARBOSA and F. H. RUDDLE, 1980 Genetic transformation of mouse embryos by microinjection of purified DNA. *Proc. Natl. Acad. Sci. USA* **77**: 7380–7384.
- HUERTAS, P., 2010 DNA resection in eukaryotes: deciding how to fix the break. *Nat. Struct. Mol. Biol.* **17**: 11–16.
- KIM, Y.-G., J. CHA and S. CHANDRASEGARAN, 1996 Hybrid restriction enzymes: Zinc finger fusions to Fok I cleavage domain. *Proc. Natl. Acad. Sci. USA* **93**: 1156–1160.
- KITADA, K., S. ISHISHITA, K. TOSAKA, R. TAKAHASHI, M. UEDA *et al.*, 2007 Transposon-tagged mutagenesis in the rat. *Nat. Methods* **4**: 131–133.
- KUEHN, M. R., A. BRADLEY, E. J. ROBERTSON and M. J. EVANS, 1987 A potential animal model for Lesch-Nyhan syndrome through introduction of HPRT mutations into mice. *Nature* **326**: 295–298.
- LEDERMANN, B., 2000 Embryonic stem cells and gene targeting. *Exp. Physiol.* **85**: 603–613.
- LI, P., C. TONG, R. MEHRAN-SHAI, L. JIA, N. WU *et al.*, 2008 Germline competent embryonic stem cells derived from rat blastocysts. *Cell* **135**: 1299–1310.
- LIEBER, M. R., 1999 The biochemistry and biological significance of nonhomologous DNA end joining: an essential repair process in multicellular eukaryotes. *Genes Cells* **4**: 77–85.
- MANI, M., J. SMITH, K. KANAVELOU, J. M. BERG and S. CHANDRASEGARAN, 2005 Binding of two zinc finger nuclease monomers to two specific sites is required for effective double-strand DNA cleavage. *Biochem. Biophys. Res. Comm.* **334**: 1191–1197.
- MARKEL, P., P. SHU, C. EBELING, G. A. CARLSON, D. L. NAGLE *et al.*, 1997 Theoretical and empirical issues for marker-assisted breeding of congenic mouse strains. *Nat. Genet.* **17**: 280–284.
- MASHIMO, T., A. TAKIZAWA, B. VOIGT, K. YOSHIMI, H. HIAI *et al.*, 2010 Generation of knockout rats with X-linked severe combined immunodeficiency (X-SCID) using zinc-finger nucleases. *PLoS One* **5**: e8870.
- MENG, X., M. B. NOYES, L. J. ZHU, N. D. LAWSON and S. A. WOLFE, 2008 Targeted gene inactivation in zebrafish using engineered zinc-finger nucleases. *Nat. Biotechnol.* **26**: 695–701.
- MISHINA, M., and K. SAKIMURA, 2007 Conditional gene targeting on the pure C57BL/6 genetic background. *Neurosci. Res.* **58**: 105–112.
- MITZUTANI, T., and A. HATTORI, 2005 New Horizon of MDRI (P-glycoprotein) study. *Drug Metab. Rev.* **37**: 489–510.
- MORTON, J., M. W. DAVIS, E. M. JORGENSEN and D. CARROLL, 2006 Induction and repair of zincfinger nuclease-targeted double-strand breaks in *Caenorhabditis elegans* somatic cells. *Proc. Natl. Acad. Sci. USA* **103**: 16370–16375.
- PARDO, B., B. GOMEZ-GONZALEZ and A. AGUILERA, 2009 DNA double-strand break repair: how to fix a broken relationship. *Cell. Mol. Life Sci.* **66**: 1039–1056.
- PIPPERT, T. R., and D. R. UMBENHAUER, 2001 The subpopulation of CF-1 mice deficient in P-glycoprotein contains a murine retroviral insertion in the *mdr1a* gene. *J. Biochem. Mol. Toxicol.* **15**: 83–89.
- PORTEUS, M. H., and D. BALTIMORE, 2003 Chimeric nucleases stimulate gene targeting in human cells. *Science* **300**: 763.
- RICH, T., R. L. ALLEN and A. H. WYLLIE, 2000 Defying death after DNA damage. *Nature* **407**: 777–783.
- RICHARDSON, C., and M. JASIN, 2000 Coupled homologous and nonhomologous repair of a double-strand break preserves genomic integrity in mammalian cells. *Mol. Cell Biol.* **20**: 9068–9075.
- SANTIAGO, Y., E. CHAN, P. Q. LIU, S. ORLANDO, L. ZHANG *et al.*, 2008 Targeted gene knockout in mammalian cells by using engineered zinc-finger nucleases. *Proc. Natl. Acad. Sci. USA* **105**: 5809–5814.
- SCHINKEL, A. H., J. J. SMIT, O. VAN TELLINGEN, J. H. BEIJNEN, E. WAGENAAR *et al.*, 1994 Disruption of the mouse *mdr1a* P-glycoprotein gene leads to a deficiency in the blood-brain barrier and to increased sensitivity to drugs. *Cell* **77**: 491–502.

- SHUKLA, V. K., Y. DOYON, J. C. MILLER, R. C. DEKELVER, E. A. MOEHLE *et al.*, 2009 Precise genome modification in the crop species *Zea mays* using zinc-finger nucleases. *Nature* **459**: 437–441.
- SMITH, J., J. M. BERG and S. CHANDRASEGARAN, 1999 A detailed study of the substrate specificity of a chimeric restriction enzyme. *Nucleic Acids Res.* **27**: 674–681.
- THOMAS, K. R., and M. R. CAPECCHI, 1987 Site-directed mutagenesis by gene targeting in mouse embryo-derived stem cells. *Cell* **51**: 503–512.
- TOWNSEND, J. A., D. A. WRIGHT, R. J. WINFREY, F. FU, M. L. MAEDER *et al.*, 2009 High-frequency modification of plant genes using engineered zinc-finger nucleases. *Nature* **459**: 442–445.
- ZAN, Y., J. D. HAAG, K. S. CHEN, L.A. SHEPEL, D. WIGINGTON *et al.*, 2003 Production of knockout rats using ENU mutagenesis and a yeast-based screening assay. *Nat. Biotechnol.* **21**: 645–651.

Communicating editor: D. A. LARGAESPADA

GENETICS

Supporting Information

<http://www.genetics.org/cgi/content/full/genetics.110.117002/DC1>

Targeted Genome Modification in Mice Using Zinc-Finger Nucleases

**Iara D. Carbery, Diana Ji, Anne Harrington, Victoria Brown,
Edward J. Weinstein, Lucy Liaw and Xiaoxia Cui**

Copyright © 2010 by the Genetics Society of America
DOI: 10.1534/genetics.110.117002

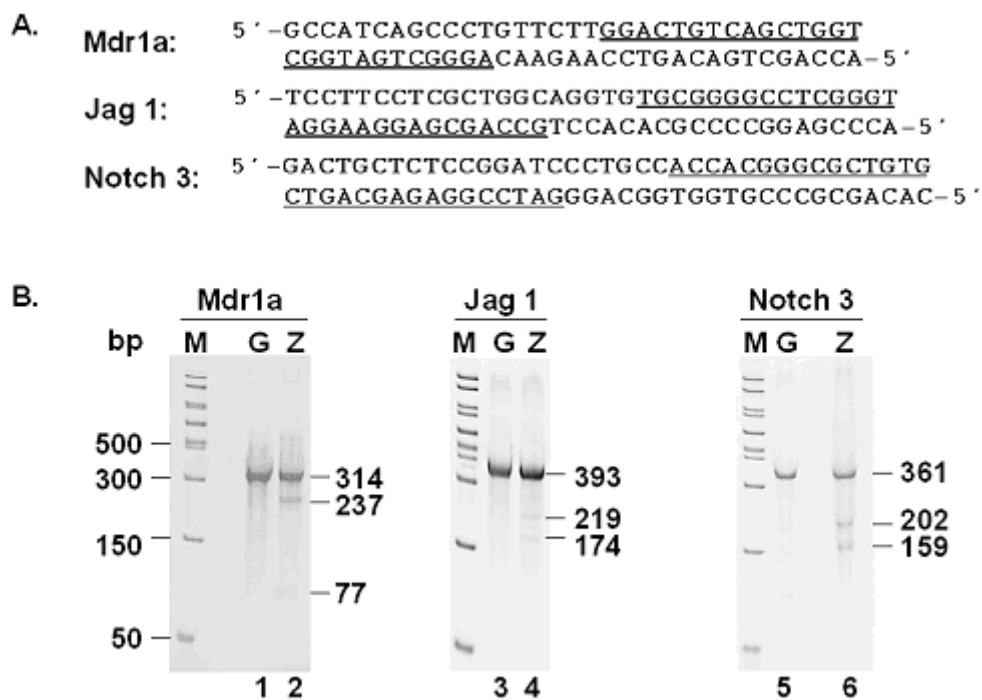


FIGURE S1.—Target sites and ZFN validation of *Mdr1a*, *Jag1*, and *Notch3*. A. ZFN target sequences. The ZFN binding sites are underlined. B. Mutation detection assay in NIH 3T3 cells to validate the ZFN mRNA activity. ZFN mRNA pairs were cotransfected into NIH 3T3 cells, which were harvested 24 h later. Genomic DNA was analyzed with the Cel-1 mutation detection assay (see Methods) to detect non-homologous end joined (NHEJ) products, indicative of ZFN activity. M, PCR marker; G (lanes 1, 3, and 5): GFP transfected control; Z (lanes 2, 4, and 6), ZFN transfected samples. Uncut wildtype and cleaved bands are marked with respective sizes in base pairs.


```
WT:      ATTTTGGCCATCAGCCCTGTTCTTGGACTGTCAGCTGGTATTTGGGCAA  
7, 17, 36: ATTTTGG-----ACTGTCAGCTGGTATTTGGGCAA  
17, 20:  ATT-----TTGGACTGTCAGCTGGTATTTGGGCAA  
34, 44:  ATTTTGGCCATCAGCCCTG-----GACTGTCAGCTGGTATTTGGGCAA
```

FIGURE S2.—The shared genotype of multiple independent F0 founders.

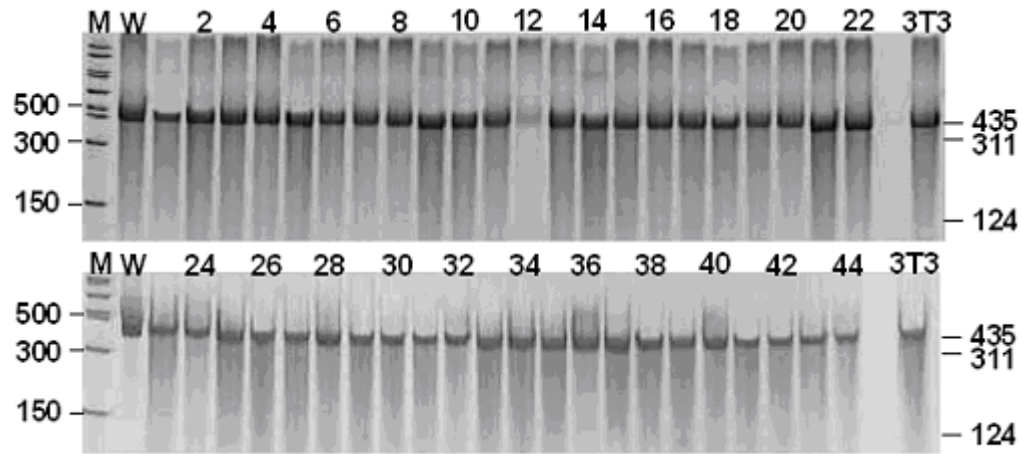


FIGURE S3.—Off-target analysis at the *Mdr1b* locus in 44 pups injected with the *Mdr1a* ZFN. M, PCR marker; WT, toe DNA from FVB/N mice that were not injected with *Mdr1a* ZFNs. 3T3, NIH 3T3 cells transfected with *Mdr1a* ZFNs as a control.

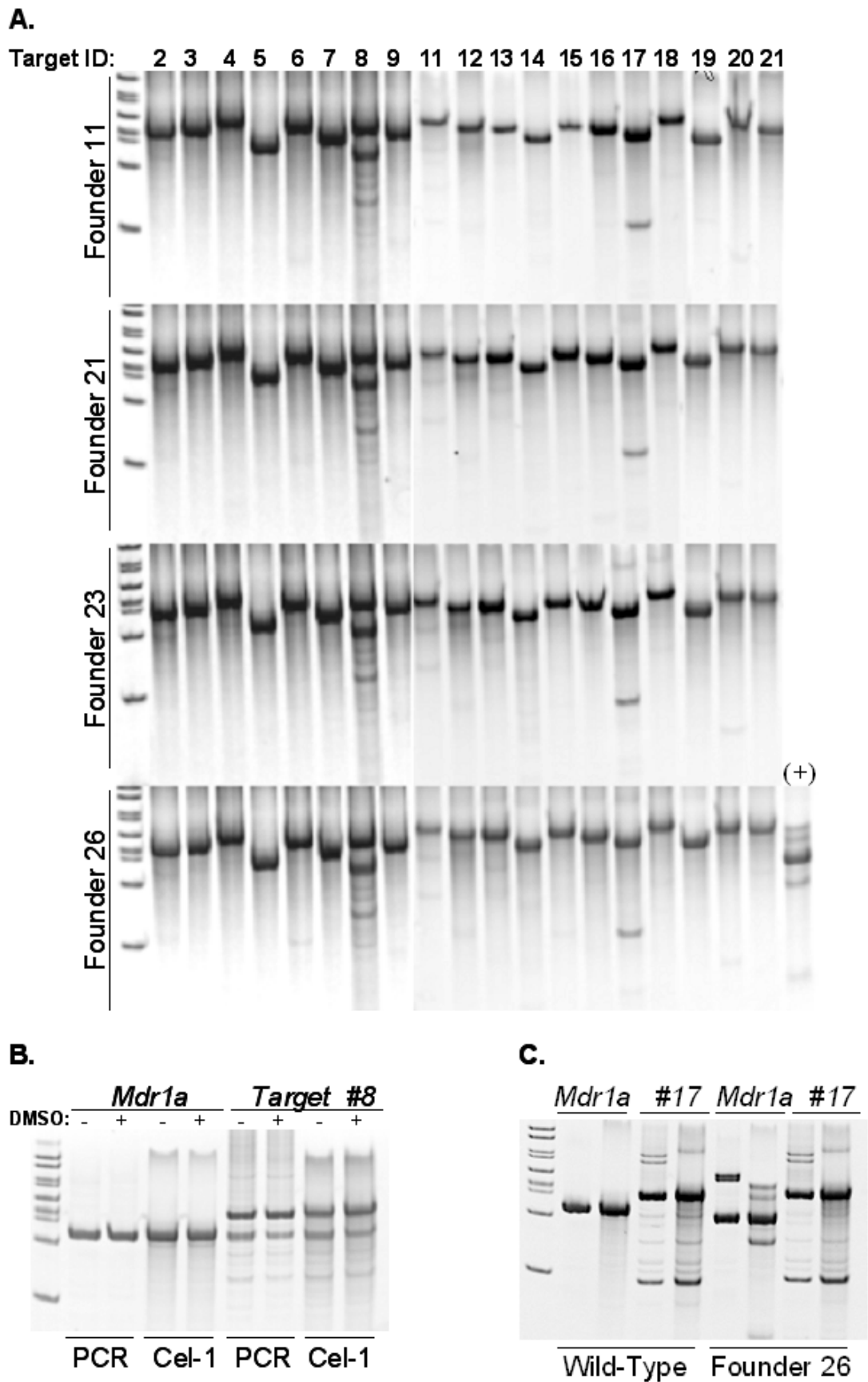


FIGURE S4.—Off-target analysis at the remaining 19 sites in four *Mdr1a* founders. Every remaining predicted potential *Mdr1a* off-target site (identified in Table S3) was tested in the 4 *Mdr1a* founders that are being maintained and bred to homozygosity (Founders 11, 21, 23, 26 described in table S1). A. Mutation detection assay at all potential off-target sites.

The Founder 26 (+) lane indicates the *Mdr1a* positive control. B. Cel-1 mutation detection analysis of wild-type mouse genomic DNA (never exposed to ZFNs) with primers specific to target #8 shows the same banding pattern for wild-type as for the founder DNA. C. PCR amplification and Cel-1 mutation detection analysis of genomic DNA from wild-type and Founder 26 animals, using primers specific to *Mdr1a* (control), and to target #17. For each gene, the left lane is the PCR product; the right lane is the PCR product treated with Cel-1 nuclease (see Methods). No differences between wild-type and founder DNA (no off-target mutations) were detected in any founder animals.

FILE S1**ZFN Validation**

Target sites for ZFNs against *Mdr1a*, *Jag1* and *Notch3* are shown in Figure S1A. *Mdr1a* on chromosome 5 is targeted in exon 7. *Jag1* on chromosome 2 is targeted at the intron 1/exon 2 junction, and *Notch3* on chromosome 17 is targeted in exon 11. ZFN activity was validated by the presence of genome modifications at each target site with a mutation detection assay (see methods) in ZFN mRNA transfected cells but not in cells transfected with a GFP-expressing plasmid as a negative control (Figure S1B).

Injection Statistics

Generally, few eggs were lost during injection. We report in table S6 the number of eggs transferred, pups born and founders identified.

TABLE S1**Summary of deletions found in *Mdr1a* targeted founders**

⁻¹⁰ ⁻⁵ ⁻² ⁺² ⁺⁵ ⁺¹⁰
GCCATCAGCCCTGTTCTTGGACTGTCAGCTGGT

ID	Deletion size (bp)+ insertion	Position	Effect on <i>Mdr1a</i> ORF
2	6 + A	-4, +2	frameshift
3	4 + C	-1, +3	in-frame
4	3	-2, +1	in-frame
5	646	-640, +6	exon skipping
6	695	-583, +112	exon skipping
7	19	-14, +5	frameshift
8	248	-238, +10	exon skipping
	417, 19	(-528- -112), (-14, +5)	exon skipping
11	533	-27, +506	exon skipping
13	392	-20, +372	exon skipping
	2	-1, +1	in-frame
	19	-14, +5	in-frame
17	19	-18, +1	in-frame
18	2	+1-+2	frameshift
19	25	-25- -1	frameshift
20	21	-15, +6	in-frame
	533	-524, +9	exon skipping
21	584	-579, +5	exon skipping
23	396	-389, +7	exon skipping
25	533	-6, +527	exon skipping
	13	-5, +8	frameshift
26	534	-516, +18	exon skipping
	75	-72, +3	in-frame
	19	-14, +5	frameshift
27	7	-2, +5	frameshift
28	731	-724, +7	exon skipping
	314	-306, +8	exon skipping
	319	-306, +13	exon skipping
29	22	-7, +15	frameshift
31	11	-4, +7	frameshift
	23	-9, +14	frameshift
	13	-6, +7	frameshift
32	9	-8, +1	in-frame
34	6	-2, +4	in-frame
36	19	-14, +5	frameshift
	430	-423, +7	exon skipping
38	28	-25, +3	frameshift
40	255	-7, +248	exon skipping

	57	-51, +6	frameshift
	19	-14, +5	frameshift
	19 + 8 (TGTCAGCC)	-4, +15	frameshift
41	11	-4, +7	frameshift
	486	-6, +480	exon skipping
42	19	-12, +7	exon skipping
	455	-451, +4	exon skipping
44	6	-2, +4	in-frame

Target site sequence schematic is illustrated at the top of the chart. ZFN binding sites are in black. The spacer in between the binding sites is in red. The positive (downstream) and negative (upstream) numbering start from the center of the spacer sequence. Predicted effect on Mdr1a ORF lists how the ORF is likely to be affected by each of the mutant alleles.

TABLE S2***Mdr1a* alleles transmitted through the germline are shown**

Founder ID	Deletion (bp)	# Hets	Wildtype	Total	% Transmission
6	small	5	2	9	77.8
	695	2			
8	small	3	0	4	100.0
	248	1			
11	417, 19	3	3	7	57.1
	533	1			
13	2	1	0	1	100.0
21	533 + 5bp	4	2	12	58.3
	47	1			
	19	1			
	21	1			
23	396	14	15	29	48.3
26	534	2	0	15	100.0
	19	8			
	11	5			
27	75	4	17	37	54.1
	19	10			
	7	6			
44	455	1	6	16	56.3
	7	1			
	6	7			

Alleles that appeared in F1 but were not originally identified in founders are highlighted in yellow.

TABLE S3**Potential off-target sites for *Mdr1a* ZFNs**

Chr. No.	Target Name	Binding Sequence	Target ID
5	Abcb1a	GCCATCAGCCCT GTTCTT GGACTGTCAGCTGGT	1
1	Pld5	GCCATCAGCtCT CAAAG AGGACTGTaAGaaGcT	2
2		GCCAAcCAGCtCT ATTTT -GGACTcTCcGCTGcT	3
3	Slc33a1	GCCATCAGCtCT ATAACA tGACTGTCTaCTGaT	4
3	Syt11	GtCAcCAaCCCT CTCCAT GGAAaGTCAGCTGGT	5
4		GaCtTCAGCCCT GACTGC tGACTGgCAaCTGGT	6
4	Anp32b	GCCAgCAGCCCT TTCCCTT GaAggGTCAGCTaGT	7
5	Pitpnm2	GCCATCAGCCCg CTCATG aGcCTGTtGCTGGT	8
5		GCCAgCAGCCCT GCCTG -GGcCTGgCAGtTaGT	9
5	Abcb1b	GCtgTCAGCCCT CTTATT GGAtTGTCAtCTGcT	10
6	Mitf	GCCcTCAGCCCT CGAGAT GctCTGTCAcCaGGT	11
7	Iqck	GCCATCAGCCCa CTGTG -GGACTtTgAGtgGGT	12
8	Kifc3	caCcTgAGCCCG CAACT -GGACTGTCAGCTGGT	13
8		cCCATCAaCaCT AACAC AGGACTGgCAcCTGGT	14
10	Oprm1	tCCAgCAGCtCT GTCTG -GGACTGTtAGaTGGT	15
10	Pcbp3	cCCAaCAGCCCT ATTAG -GGACaGgCAcCTGGT	16
11		GCCATCAGgCaT GGAGA -GGACatTCAGCTGGa	17
12		GCCATCgcCCCT GGCCT -GGAtgGTCtGCTGGT	18
12		cCCATCAGCaCT GTGGAC GGtCgGTCAtCTGGT	19
15		GCCAggAGCCt TCAAGT GGACTGTCAGtTGcT	20
16	Etv5	GCCAgCAGCtgT GACTGT GGgCTaTCAGCTGGT	21

Twenty sites in the mouse genome that are most similar (with \leq five mismatches) to the *Mdr1a* target site are shown. Listed are the numbers of the chromosomes they are on and gene names if known. All the mismatched bases are in lower case. The spacer sequence between the binding sites is in bold letters. Sites in antisense orientation are highlighted in grey.

TABLE S4
Potential off-target sites for *Jag1* ZFNs

Chr. No.	Binding Sequence	No. Mismatch	Target Name
2	GACCCGAGGCCCCGCA CACCT -GCCAGCGAGGAAGGAA	0	Jag1
4	TcCCCGAGGaCCtGgg ACCCT -GCCAGgGAGGAAGGAG	6	Rnf220
1	GACCCGAGGCCatGCA AAATGT GCCAGtcAGGgAGaAC	6	
11	GaaCTTtCgCGCcGGCT TGCGAGT GC GG GGCcCGGcTG	7	Adams2
11	CACCCGcGGCCCCcCA CGCCGG GaCAGCGAtGcgtGAG	7	Ccnjl
11	AACcTGAGaCtCtGC ATTTCTG CCAGCaAcGcAGGAG	7	
15	CTgCTTCCgCtgTGGCT TTCTTCT GtGGGGtCTCGGGaC	7	Eif3eip
3	CagCTTCCCTCGCgc GCGCGGG cGCGGGGCTgGGGcT	7	Kcnd3
10	CACCCaAGGCCatGtg CAGGT -aCCAcCGAGGAAGGAC	7	
16	TgCaaGAGaCCCCG CAGTTTTT GcTAgAGAGGAAGaAT	7	
16	CACCGAaGCCagGC AGGCCAT GCaAGgaAGGAAGGAA	7	Col8a1
8	CTCCTTCCcCGgTgT CTCCA -TGgGtGaCtTCGGGTG	7	
9	GcCCTTgtTcCCTGGCT TCTTC -TGtGGGGaCTCaGGTT	7	Clstn2
4	CACCCcAGGgCCgGCA AGATGG cCCAGCGgGtAAaGAT	7	
4	GTCaTTcCtCGCTGcg GAATC -TGaGGGGCCTCtGGTA	7	
14	GTCCTTCCtCtCTGGCT TGGGGT GgaGGGtgagGGGTG	7	
18	TTCCaTCtTCtCaGGC AACAAGT GCGGGtCCTtaGGTC	7	Isoc1
18	GTagTTCCCTgagTGGC AGACA -TGcTGGGCCTCaGGTG	7	Myo7b
1	CTCCTgCCTCaCTaGCT TCCCC TGcTGGcCaCGGcTC	7	
1	GTCCCTgagTgGCTGGCT TCAGCCT GtGaGGCCaCGGGTG	7	Ush2a
1	CACCCccaGCCCCCa AAAGAAA cCCAGaGAGGAAGGAT	7	
1	AAgCCGAGGCCCCGcG GCCATG aaCgGCaAaGAAGGAC	7	
1	GAaCCGAGGCCtCGC AGGTTT -cCCAGgGcacAAGGAC	7	Ankrd39
1	ATCCTTCCtCtCctCT TGGGA -aGaGGGGCCTCGGGgG	7	
7	GatCaTCaTCGCTcGCT TGCAGG gGCGGGGCCgCGGGTA	7	Bax
7	CTgCTTCCCTCGCTGt CTGGTCT GCatGcCCTaGGGTA	7	
7	GTCCTaCtTCcCaGGC CTTTTGT GtGGGGCCTCcGtTT	7	
13	TtCCaGgGGCtCtGC AGCAAA AGCCAGtGAGGAAtGAC	7	Cap2
13	TtCCaGAtGCCtCGC AGTTCT -GCCAGtGAGGAcGGcG	7	Zcchc6
13	CACCCacGGCCtGCAT TGTTT -GgaAGgGAGGgAGGAG	7	
2	GACCCGAGGCCCCGcG GCTCAC cCCAGgcAGccAGGcA	7	Vps39
5	CACCCcAGGCCCaCcC AGCTATG CaAGCaAGGAAGcAT	7	Srpk2
5	CTCCTaCtTgGCTGGCT TGTG -TGCaGtGcTtGGGTT	7	Chst12

Chromosome number, potential sites, number of mismatches, and gene names (if known) are listed. All mismatched bases are in lower case. The spacer sequence between the binding sites is in bold. Sites in antisense orientation are highlighted in grey.

TABLE S5
Potential off-target sites for *Notch3* ZFNs

Chr. No.	Binding Sequence	No. Mismatch	Target Name
17	ACACAGCGCCCGTGGT GGCAGG GATCCGGAGAGCAGTC	0	Notch3
12	GCtCgGCGtCtGgGGT TTTAC -GATCa-GAGAGCAGTC	6	
10	TCACAGtGCCCaGGTA AATTG -GATCaGAcAaaAGTCC	7	
10	AcACTaCcCTCtGgg CCCTT -ACCACGGGCGCTGTtT	7	
10	ACACAGCcCCtGTGGT GTACA -GATCCGAtacaCAtTC	7	Bicc1
5	TCACActGCCccaGT GGCTTA tATCaGAAGAGCAGTC	7	
5	ACACAGCcCaCaGaGGT TGACAG tTCCtGAGAGCtGTC	7	Tmem132c
1	AGcCaGgTCTTCGGAT CCTAGC ACCcAGatGCTGTGT	7	Inpp5d
19	AGgtTGtcCTCtGATC ACCTG -cCCACGGGcCTGTGG	7	Golga7b
8	CCACAGaGCCctgGaa GGAGCT GATcGCAGAGCAGcC	7	
8	ACAgAGCatCCcTGGT ACATGT GgTCCaCAGAGCAfTC	7	
8	GCACAGCcaCCGTGGT GACTCA eAtTCGtGAGCcGTtT	7	Wwox
9	TCACAGatCCtGTGGT TCTGA -aATCCagGAGCAGTtT	7	
9	TttaAGCaCCCGTGGT TTGAGG AgCCGgGAGCAGcCT	7	Vps13c
12	CCACAGacCCCcTgCt GCAAA -GtTCCGAGAGCAGcaG	7	
12	AGcCTGaTCTaGGATg ACAAC -ACCgCaGGaGCTGTGC	7	Smoc1
12	AGACTGCTCTtGGgTC CCGGG -gCCACctGCcCTGTaC	7	
4	cACTcaTCTTcATg GGGATA ACCACGGGaGCTGTGG	7	
4	ACACAGgGCCtGTGcT TCCTT -GATtCtAAGAGaAGgC	7	Gm1027
3	GGAgTGCTCagtGAg CCTGACC tCCACGGGcCtGTGC	7	
3	GgCTGCTCTTCaGt TCCTGTAT gCtAaGGGcCtGTGC	7	
13	TCtCAtgtCCCGTGGT CTGAT -GATCaaTAGAaCAGTC	7	Serinc5
2	CCACtGCcCCCcTGGT CCTTTG GATCtGGgccGCAGTC	7	Itgav
2	GACTcCTCaAaGGATC TCTGC -AagACaGGtGCTGTGT	7	Msrb2
2	GACTGCcCTCCGGga CCCTGG AgCCAgGGGaGCTaTGG	7	Rapgef1

Chromosome number, potential sites, number of mismatches, and gene names (if known) are listed. All mismatched bases are in loser case. The spacer sequence between the binding sites is in bold. Sites in antisense orientation are highlighted in grey.

TABLE S6**Injection statistics**

Target	Strain	Eggs transferred	Pups born	Founders
<i>Mdr1a</i>	FVB/N	100	44	34
<i>Jag1</i>	C57BL/6	117	38	8
<i>Jag1</i>	FVB/N	102	17	4
<i>Notch3</i>	FVB/N	103	41	8